

A Diffusion Model for Arsenic in Silicon

Abstract: It is proposed that double acceptor-level vacancies are responsible for arsenic diffusion into silicon. A computer program, which combines this diffusion mechanism with the formation of arsenic clusters and an internal electric field induced by the impurity gradient, is used to calculate arsenic diffusion profiles in wide ranges of diffusion temperatures and surface impurity concentrations. The calculated diffusion profiles are in good agreement with the measured profiles.

Introduction

Masters et al. [1] have experimentally demonstrated that arsenic diffusivity increases with the electron concentration in silicon below 10^{20} electrons/cm³. This experimental result can be explained by diffusion via a single-level vacancy mechanism [2]. By applying Boltzmann-Matano analysis to numerous arsenic diffusion profiles, Kennedy [3] recently observed that arsenic diffusivity increases with the electron concentration to a maximum value and then decreases monotonically. To explain this diffusivity decrease with increasing electron concentration, Hu [4] proposed the formation of arsenic clusters in a study based on vapor pressure measurements. However, Kennedy's diffusivity vs electron concentration curve cannot be predicted by combining the mechanisms of cluster-formation and single-level vacancy diffusion. Watkins [5], in his electron paramagnetic resonance measurements, indicated the existence of the double negative state (or the second acceptor state) vacancy. This paper proposes a modified arsenic diffusion model that integrates Hu's cluster mechanism into the double-level vacancy diffusion mechanism.

Analysis

The Shockley-Last theory [6] indicates that the ratio of concentrations of flaws in any one of the charge states follows the relationship:

$$f_{0v} : f_{1va} : f_{2va} = 1 : \exp[(E_F - E_{1va})/kT] : \exp[(2E_F - E_{1va} - E_{2va})/kT], \quad (1)$$

where f_{0v} = the fraction of the neutral vacancies,
 f_{1va} = the fraction of the first acceptor-level vacancies,
 f_{2va} = the fraction of the second acceptor-level vacancies,
 E_F = Fermi level,
 E_{1va} = first acceptor level of vacancies,
 E_{2va} = second acceptor level of vacancies,
 k = Boltzmann's constant, and
 T = absolute temperature in degrees Kelvin.

The ratio f of the total vacancy concentration in the extrinsic silicon to that in the intrinsic silicon is given by

$$f = \left(1 + \exp\frac{E_F - E_{1va}}{kT} + \exp\frac{2E_F - E_{1va} - E_{2va}}{kT}\right) \times \left(1 + \exp\frac{E_i - E_{1va}}{kT} + \exp\frac{2E_i - E_{1va} - E_{2va}}{kT}\right)^{-1} \\ = \left[1 + \left(\frac{n}{n_i} \exp\frac{E_i - E_{1va}}{kT}\right) \left(1 + \frac{n}{n_i} \exp\frac{E_i - E_{2va}}{kT}\right)\right] \times \left[1 + \left(\exp\frac{E_i - E_{1va}}{kT}\right) \left(1 + \exp\frac{E_i - E_{2va}}{kT}\right)\right]^{-1}, \quad (2)$$

where E_i = the intrinsic Fermi level,
 n = electron concentration in the extrinsic silicon, and
 n_i = electron concentration in the intrinsic silicon, which is a function of temperature [7] as shown in Fig. 1.

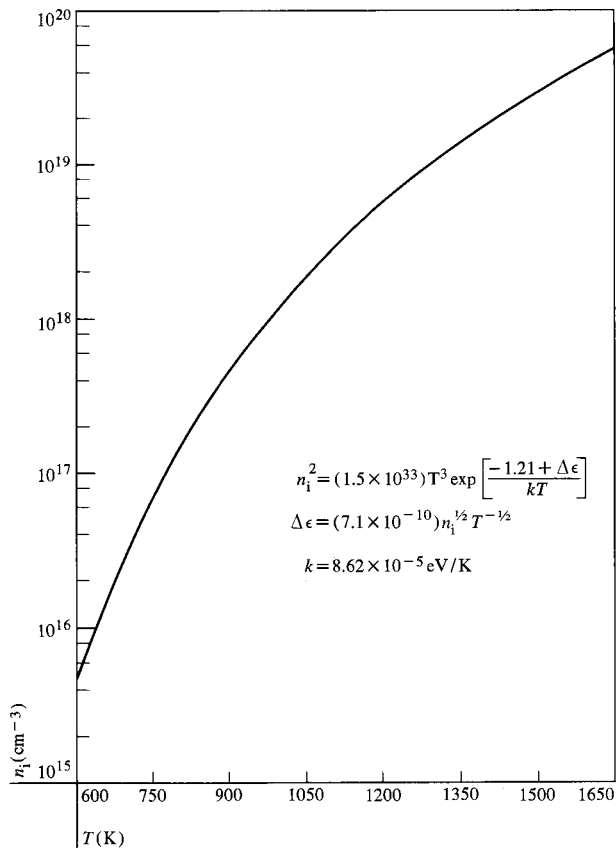


Figure 1 n_i vs T .

By taking the approximation that the diffusivity is proportional to the total vacancy concentration [8,9], the ratio of diffusivity in extrinsic to intrinsic silicon is proportional to the factor f given in Eq. (2). The effect of the internal electric field on the diffusivity introduces an additional multiplication factor h [10] to the diffusivity:

$$h = 1 + N_D [N_D^2 + (2n_i)^2]^{-1/2}, \quad (3)$$

where N_D = arsenic concentration.

Hu's cluster mechanism [4] also gives a multiplication factor g to the diffusivity:

$$g \approx \left\{ 1 + 32 A \exp[\Delta H/kT] \times \left[\frac{1}{1 + \frac{1}{2} \exp[(E_{As} - E_F)/kT]} \right]^4 \left(\frac{N_{As}}{N_S} \right)^3 \right\}^{-1}, \quad (4)$$

where A = configurational multiplicity,
 N_S = concentration of lattice sites,
 N_{As} = concentration of monatomic arsenic, and
 E_{As} = monatomic arsenic energy level.

Since g approaches 1 at low arsenic concentration and N_{As} approaches n at the diffusion temperature, Eq. (4) can be rewritten as

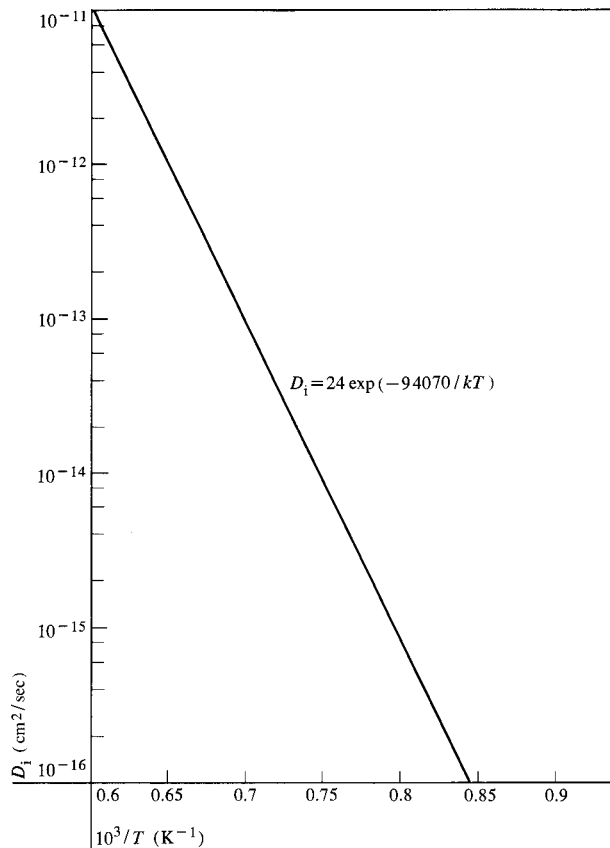


Figure 2 D_i vs $1000/T$.

$$g \approx [1 + C \exp[\Delta E/kT] (n/n_i)^3]^{-1}, \quad (5)$$

where C and ΔE are the new lumped constants. By combining these factors, the ratio of the diffusivity in extrinsic to intrinsic silicon D/D_i is given by

$$\begin{aligned} \frac{D}{D_i} &= fgh \\ &= \left[1 + \left(\frac{n}{n_i} \exp \frac{E_i - E_{1va}}{kT} \right) \left(1 + \frac{n}{n_i} \exp \frac{E_i - E_{2va}}{kT} \right) \right] \\ &\times \left[1 + \left(\exp \frac{E_i - E_{1va}}{kT} \right) \left(1 + \exp \frac{E_i - E_{2va}}{kT} \right) \right]^{-1} \\ &\times \left[1 + C \left(\exp \frac{\Delta E}{kT} \right) \left(\frac{n}{n_i} \right)^3 \right]^{-1} \\ &\times \{ 1 + N_D [N_D^2 + (2n_i)^2]^{-1/2} \}. \end{aligned} \quad (6)$$

In the derivations above, nondegenerate statistics have been used. The error thus introduced is no more than 15%, because of the extremely high intrinsic electron concentration at the diffusion temperature. In order to determine the unknown constants in Eq. (6), numerous arsenic diffusion profiles on $\langle 100 \rangle$ silicon, obtained by neutron activation analysis, were matched numerically. The intrinsic diffusivity D_i shown in Fig. 2 is obtained from low-concentration arsenic diffusion profiles:

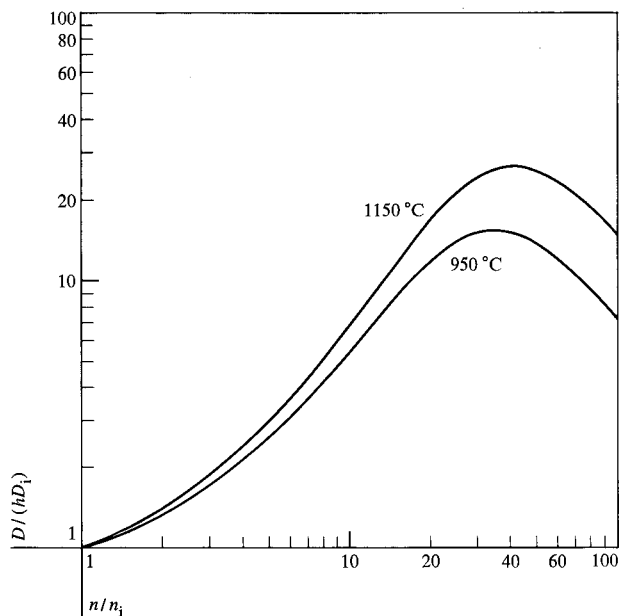
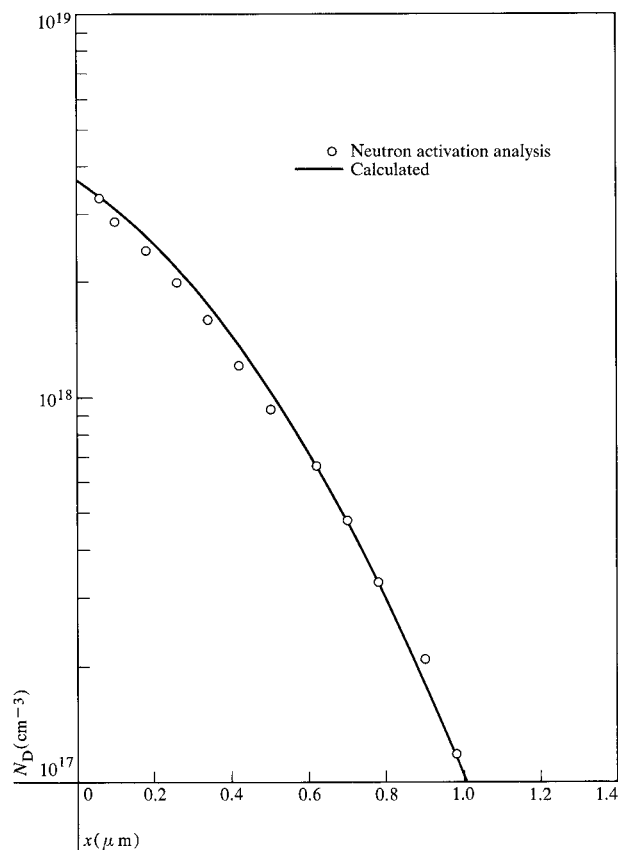


Figure 3 D/hD_i vs n/n_i .

Figure 4 Arsenic doping profile for $T = 1200^\circ\text{C}$, $t = 60$ min.



474

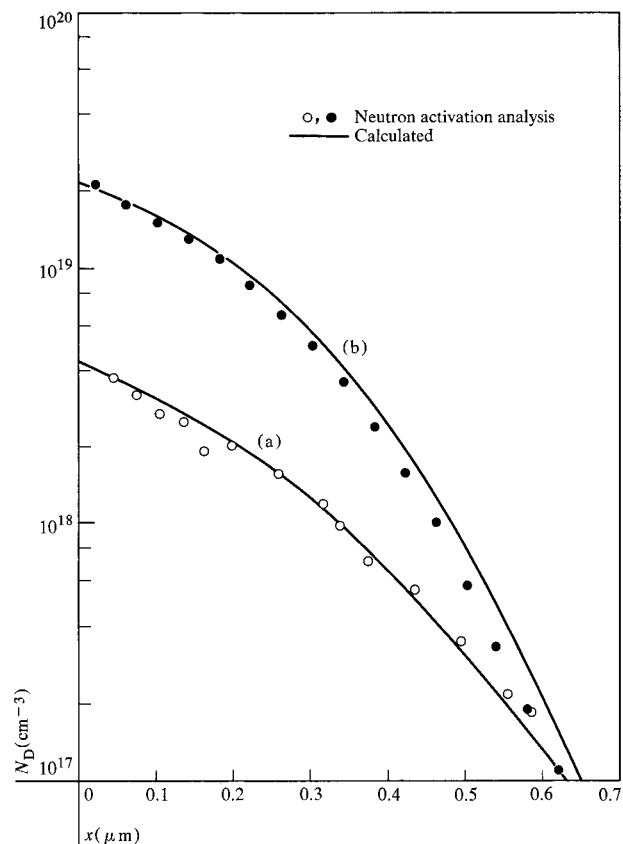


Figure 5 Profiles for $T = 1108^\circ\text{C}$, (a) $t = 200$ min; (b) $t = 2$ h.

$$D_i = 24 \exp - (94070^*/kT). \quad (7)$$

It is noted that for low-concentration arsenic diffusions, since the factors given in Eqs. (2), (3), and (5) are unity, the intrinsic diffusivity D_i is a function of temperature only. From matching the arsenic diffusion profiles in wide ranges of temperature and surface concentration, the following constants are found:

$$\begin{aligned} E_i - E_{1va} &= -2300 \text{ cal/mol;} \\ E_i - E_{2va} &= -6200 \text{ cal/mol;} \\ C &= 3.159 \times 10^{-6}; \text{ and} \\ \Delta E &= 5580 \text{ cal/mol.} \end{aligned}$$

It is observed that the acceptor levels of the vacancies in silicon given in Eqs. (8) are the values at the diffusion temperature. At room temperature, the first and second acceptor levels of the vacancies in silicon are estimated to be at 0.44 and 0.21 eV, respectively, below the conduction band edge.

Comparison between theory and experiments

With constants from Eq. (8), $D/(hD_i)$ from (6) is plotted in Fig. 3. Profiles calculated by computer using Eqs.

*cal/mol

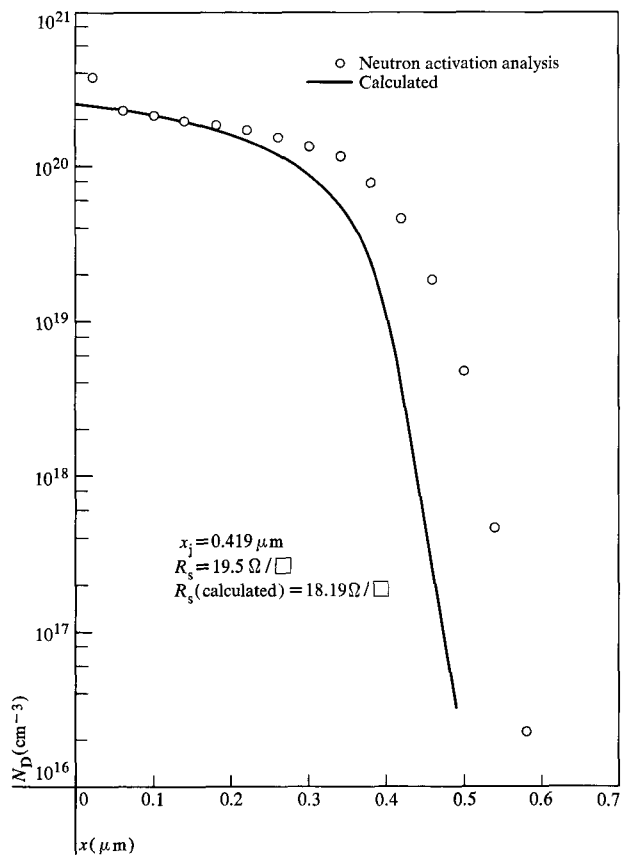


Figure 6 Profile for $T = 1050^\circ\text{C}$, $t = 60$ min.

(6) through (8) are compared with the corresponding profiles measured by neutron activation analysis in Figs. 4 through 9. The sheet resistivity of some of these profiles is also calculated from the resistivity data given in Ref.[11]. In Figs. 6 and 8, it should be observed that the junction depth measurements are in better agreement with the calculated profiles than with the measured profiles. In general, the calculated and measured profiles are in good agreement.

It should be noted that the concentration profile calculated as a solution from the diffusion model is a total concentration, since at diffusion temperature all impurities are assumed to be completely ionized. Hence, such profiles should be compared with experimental profiles from radiochemical analysis or neutron activation. For consistency, the concentration for the resistivity data in Ref.[11] has also been kept as a total concentration. For computation of device characteristics, the profile from the diffusion model must be corrected to obtain an ionized or electrically active concentration profile. However, since the concentration within a diffusion length from the junctions is low enough to be treated as completely ionized, the use of the model described in this paper has produced satisfactory agreement between com-

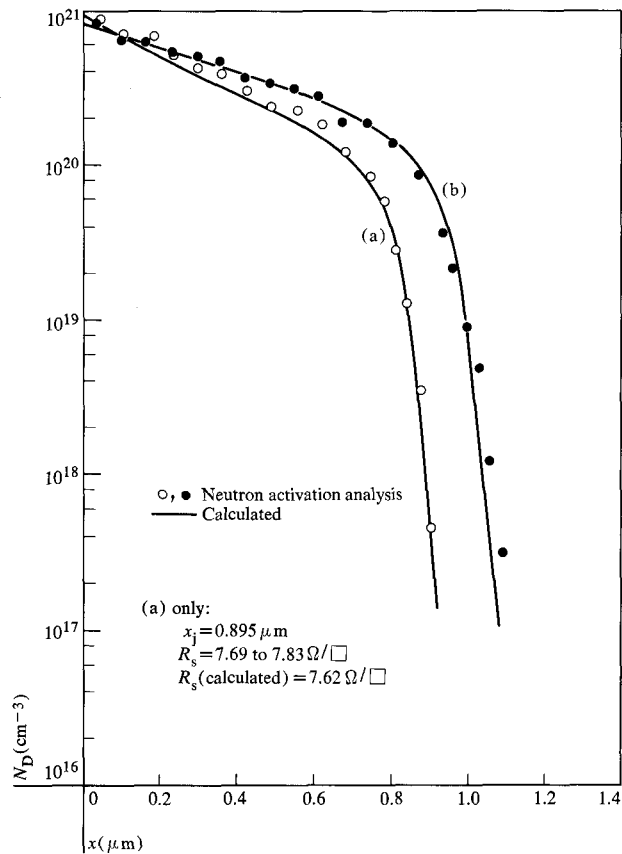
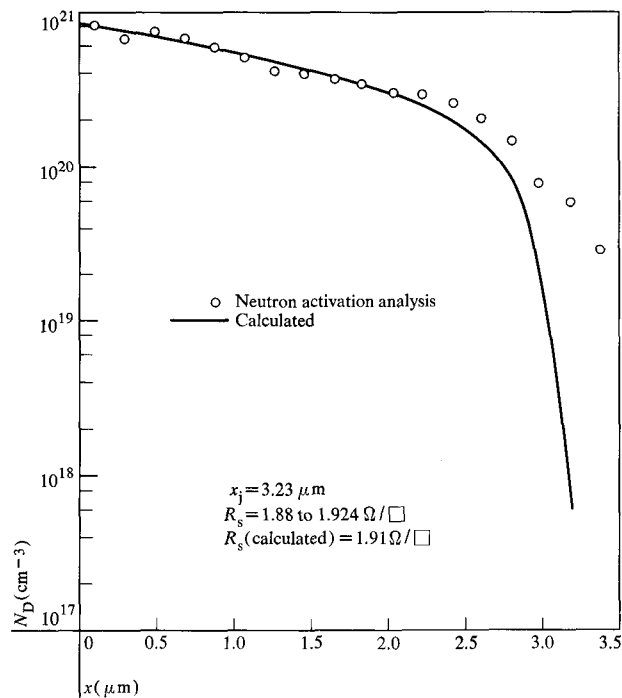


Figure 7 Profiles for (a) $T = 950^\circ\text{C}$, $t = 28$ h; (b) $T = 1000^\circ\text{C}$, $t = 8$ h 25 min.

Figure 8 Profile for $T = 1050^\circ\text{C}$, $t = 19$ h.



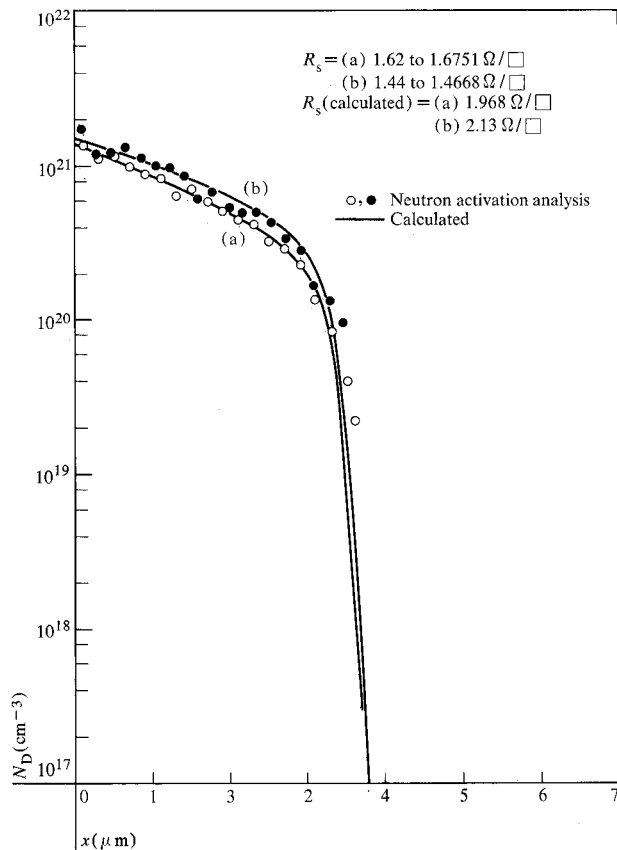


Figure 9 Profiles for (a) $T = 1100^\circ\text{C}$, $t = 5\text{ h } 30\text{ min}$; (b) $T = 1150^\circ\text{C}$, $t = 1\text{ h } 40\text{ min}$.

puted and measured transistor characteristics over wide ranges of operating levels and geometries.

Acknowledgments

The authors thank F. Keicher, R. Kastl, J. Makris, and K. Kroell for many of the measurements used in the development of the model.

References

1. B. J. Masters and J. M. Fairfield, *J. Appl. Phys.* **40**, 2390 (1969).
2. S. M. Hu, *Phys. Rev.* **180**, 773 (1969).
3. D. P. Kennedy and P. C. Murley, *Proc. IEEE* **59**, 335 (1971).
4. S. M. Hu, Chapter 5 in *Atomic Diffusion in Semiconductors*, D. Shaw, Ed., Plenum Press, London 1972, to be published.
5. G. D. Watkins, *Proc. 7th Int. Conference on the Physics of Semiconductors*, Paris 1964, vol. III, pp. 97-113.
6. W. Shockley and J. T. Last, *Phys. Rev.* **107**, 392 (1957).
7. F. J. Morin and J. P. Maita, *Phys. Rev.* **94**, 1525 (1954); *Ibid.* **96**, 28 (1954).
8. M. W. Valenta and C. Ramasastry, *Phys. Rev.* **106**, 73 (1957).
9. M. F. Millea, *J. Phys. Chem. Solids* **27**, 315 (1966).
10. F. M. Smits, *Proc. IRE* **46**, 1049 (1958).
11. T. L. Chiu and H. N. Ghosh, *IBM J. Res. Develop.* **15**, 477 (1971, this issue).

Received April 16, 1971

The authors are located at the IBM Components Division Laboratory, E. Fishkill (Hopewell Junction), New York 12533.